VIP NMR Porosity Screening Very Important Paper

DOI: 10.1002/ange.201305247

Ex Situ NMR Relaxometry of Metal–Organic Frameworks for Rapid Surface-Area Screening**

Joseph J. Chen, Xueqian Kong, Kenji Sumida, Mary Anne Manumpil, Jeffrey R. Long, and Jeffrey A. Reimer*

Metal–organic frameworks are porous crystalline solids consisting of metal clusters or ions connected by organic linkers. These frameworks can exhibit exceptional gas-storage capacities and adsorptive selectivities;[1] these properties have led to their investigation for a vast number of applications.[2] However, optimization remains difficult because the number of metal–ligand combinations is effectively infinite and because a large number of phases can emerge for even a single choice of metal and ligand. Synthetic reaction conditions play a crucial role in determining which phase precipitates from solution. Thus, preparation of the desired material in a pure, crystalline form relies on extensive systematic screening of many reaction parameters.[3] The modular nature of the solventothermal preparation of metal–organic frameworks makes high-throughput synthesis an effective means for rapidly exploring the parameter space.[4] However, the subsequent characterization of new compounds becomes a bottleneck for this type of workflow since structural characterization by XRD or evaluation of the BET surface area through adsorption measurements are not practical for large numbers of unknown samples. Thus, the development of a tool to analyze porosity that precludes the need to perform labor-intensive tasks (i.e. activation and sorption measurements) on each sample would greatly accelerate the discovery of potentially interesting frameworks by quickly eliminating nonporous or low-surface-area materials that are not of interest.

Nuclear magnetic resonance (NMR) relaxometry can potentially provide an initial estimate of the pore volume and surface area of an unknown metal–organic framework. These methods use imbibed fluid nuclei as probes of the internal surface area and have been used extensively to characterize porous media, including rocks, silica, zeolites, cements, and soils.[5] Transverse relaxation (T_2) is a process in which observable magnetization decays to equilibrium in an exponential fashion.[6] The relaxation rate of liquid nuclei imbibed in porous media generally depends on the degree of confinement because of interactions with the pore walls[7] and internal field gradients.[8] Although some relaxation studies of hydrocarbon gases in MOF-5 and $Cu_3(BTC)_2$ (BTC = benzene-1,3,5- tricarboxylic acid) have been conducted,[9] the relaxation behavior of liquids in metal–organic frameworks and its connection to internal surface area has yet to be studied systematically.

Herein, we demonstrate a correlation between the BET surface area and the transverse relaxation (T_2) of solvent-imbibed metal–organic frameworks and zeolites. The use of a liquid probe greatly simplifies sample preparation to washing and filtration, thereby minimizing the amount of necessary automation hardware while eliminating the time-consuming process of sample isolation and activation. Furthermore, the relaxation measurements described in this study can be performed considerably faster than a typical BET surface area measurement. Lastly, the integration of autosampling hardware allows large numbers of samples to be screened without the need for manual sample transfer or instrument operation, thus providing a convenient initial screening method well-suited for integration into a high-throughput workflow (see Figure S8 in the Supporting Information). Note that this technique does not replace adsorption-based characterization experiments, but should facilitate the identification of a generally small fraction of highly porous materials within a combinatorial library of unknown samples, thereby allowing researchers to perform time-consuming workup on the most promising frameworks.

Samples of solvent-imbibed metal–organic frameworks can be approximated as having two pore size regimes, as shown in Figure 1 a and b using Mg_2(dobdc) (Mg-MOF-74, CPO-27-Mg; $dobdc^{4-}$ = 2,5-dioxido-1,4-benzenedicarboxylate) as an example: nanometer-sized pores belonging to the inherent structure of the framework (intraparticle) and micrometer-sized voids between the individual crystallites (interparticle). Since solvent molecules are expected to diffuse slowly between the two types of pores, relaxation should exhibit multiexponential behavior, where faster relaxation occurs for intraparticle solvent and slower relaxation for interparticle solvent (Figure 1 c). An algorithm referred to as an inverse Laplace transform (ILT) or Laplace inversion deconvolutes multiexponential transverse relaxation into individual exponential components (Figure 1 d).[10] As shown in Figure 2, the T_2 "relaxation spectra" of dimethyl sulfoxide

[*] J. J. Chen,[+] Dr. X. Kong,[+] Dr. J. A. Reimer
Department of Chemical and Biomolecular Engineering
University of California, Berkeley, CA, 94703 (USA)
E-mail: joseph.chen@berkeley.edu
Dr. K. Sumida, M. A. Manumpil, Dr. J. R. Long
Department of Chemistry
University of California, Berkeley, CA, 94703 (USA)
[+] These authors contributed equally to this work.

[**] The information, data, or work presented herein was funded by the US Department of Energy, Advanced Research Projects Agency-Energy (ARPA-E) under Grant No. DE-AR0000103. We acknowledge J. A. Mason and A. Milner for assistance with the sample preparation, and Fulbright New Zealand for partial support of K.S. The Laplace inversion software is used courtesy of the Victoria University of Wellington.

Supporting information for this article is available on the WWW under http://dx.doi.org/10.1002/anie.201305247.

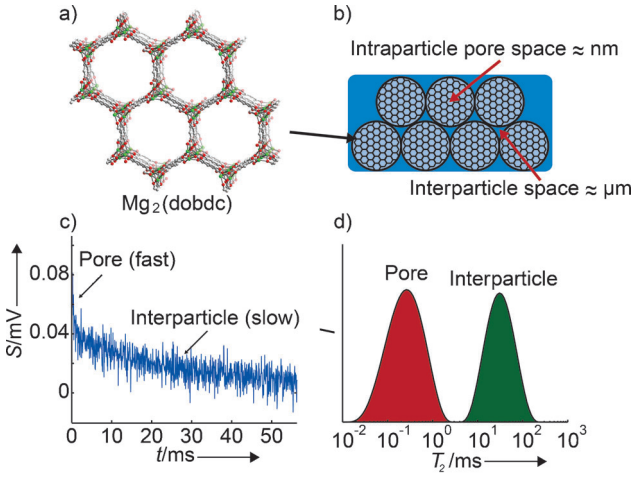

Figure 1. Illustration of the multiple length scales that generate multi-exponential relaxation in Mg_2(dobdc). a) A portion of the crystal structure of Mg_2(dobdc). Green, gray, and red spheres represent Mg, C, and O atoms, respectively, while H atoms are omitted for clarity; b) length scales formed by packed porous particles; c) NMR signal (S) versus time (t) showing relaxation with slow and fast exponential decays; and d) Laplace inversion of relaxation data with two relaxation populations corresponding to pore and interparticle solvent.

(DMSO) protons imbibed in Mg_2(dobdc)[1] (Figure 1a; $SA_{BET} = 1660\ m^2\,g^{-1}$) exhibits multiexponential relaxation for a series of solvent contents. Note that DMSO was chosen as a probe solvent because of its common use in the synthesis of metal–organic frameworks and its inert nature towards most compounds. Relaxation measurements were conducted on samples with known amounts of solvent using the single-sided NMR-MOUSE (MObile Universal Surface Explorer) setup, which measures the ^{1}H NMR signal of samples placed outside the magnet,[11] thus simplifying the incorporation of automation hardware. T_2 relaxation was measured using a CPMG sequence[12] with an approximate experiment duration of 15–30 min.

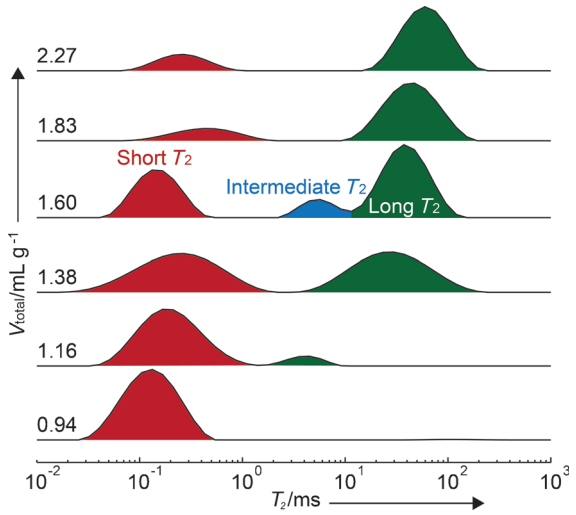

Figure 2. Profiles of T_2 relaxation times, or "relaxation spectra," for Mg_2(dobdc) with various amounts of DMSO added (V_{total}). Solvent content is normalized to the mass of the evacuated framework. Relaxation times can be roughly grouped into short, intermediate, and long T_2 regimes. The total intensity at each solvent content is normalized to unity.

At low solvent content, a single signal appears which represents a population of solvent with a short T_2 value (ca. 10^{-2} to 10^0 ms). As a result of the short relaxation times compared to neat DMSO ($T_{2,DMSO} \approx 300$ ms on the NMR-MOUSE), the protons associated with this relaxation population reside on solvent molecules confined within the one-dimensional channels of Mg_2(dobdc). The presence of a single population indicates that little solvent exists in the interparticle voids, which can be attributed to the much stronger solvent binding expected within the confines of the pores compared to the voids between the individual particles. As solvent is added, a second population appears at longer T_2 values (10^0 to 10^3 ms), and the corresponding relaxation signal shifts to longer times. Since the pores are completely filled at higher solvent contents, this signal can be assigned to interparticle solvent. Successive solvent addition leads to a greater proportion of molecules that interact weakly with the framework, thus causing the relaxation time to approach the value for neat DMSO. Notably, a third intermediate relaxation population occasionally appears with intermediate relaxation times (10^0 to 10^1 ms). This range of relaxation times also corresponds to that for the long T_2 signals at lower solvent content, which suggests that the intermediate relaxation signals correspond to solvent localized near the surface of the particles rather than inside the framework pores. Sufficiently fast diffusional exchange between the pores and interparticle space during the NMR experiment would indeed generate an intermediate relaxation environment, as discussed below. Furthermore, each relaxation population is represented by broad signals that span orders of magnitude, and given the low signal-to-noise ratio associated with using the NMR-MOUSE setup and the uniform pore size of metal–organic frameworks, the breadth of the spectrum represents an uncertainty originating from experimental noise rather than the existence of a wide distribution of pore sizes.

Since the signal area in the relaxation spectrum is proportional to the number of spins (i.e. solvent volume) of that relaxation population, a connection can be made between the pore volume and the relaxation behavior. The surface area in microporous media is roughly proportional to the pore volume, and frameworks with high surface areas should exhibit relaxation spectra with proportionally larger short T_2 signals at a given solvent content. Indeed, the relaxation behavior for a variety of other samples, including low-surface-area zeolites, metal–organic frameworks with paramagnetic metal centers (e.g. Ni_2(dobdc)[13]), or frameworks with higher dimensionality pores (e.g. UiO-66[14]), remains qualitatively similar to that for Mg_2(dobdc) (see the Supporting Information).

The fraction of total intensity encompassed by the short T_2 signal corresponding to the solvent molecules within the micropores is shown in Figure 3 for Mg_2(dobdc) and a low-surface-area zeolite Na-mordenite ($SA_{BET} = 398\ m^2\,g^{-1}$). Note that the short T_2 signal is defined as the fastest relaxation population in the "relaxation spectra" displaying multiple signals. Spectra with single signals are classified as belonging

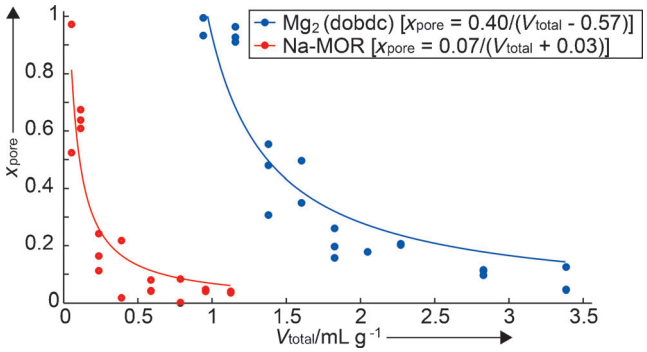

Figure 3. Decay of the fraction of total intensity (x_{pore}) encompassed by the pore-confined solvent plotted versus increasing solvent content (V_{total}). The solid lines indicate the fits of the data with Equation (1). Na-MOR is the zeolite sodium mordenite.

to either solvent within the pores or within the bulk liquid, depending on the magnitude of the relaxation times. The fraction of total signal associated with pores (x_{pore}) should be equal to the ratio of the normalized pore volume to the normalized total solvent content (V_{pore}/V_{total}). However, a small amount of strongly bound immobile solvent may go undetected because of the extremely short relaxation times that these nuclei exhibit ($T_2 \approx 10\ \mu s$). Therefore, the ratio for x_{pore} must be modified according to Equation (1).

$$x_{pore} = \frac{V_{pore} - V_{im}}{V_{total} - V_{im}} \quad (1)$$

V_{im} represents the normalized volume of immobile solvent, and the fits of Equation (1) are shown in Figure 3. For Mg_2(dobdc), V_{im} is relatively large, while for Na-MOR, the V_{im} value is small (and positive due to experimental noise), which indicates that Mg_2(dobdc) binds solvent more strongly than Na-MOR, most likely because of the presence of open metal sites in Mg_2(dobdc). Figure 4 shows the correlation between V_{pore} and the experimental nitrogen BET surface area for a variety of porous materials imbibed with DMSO. *N*,*N*-Dimethylformamide (DMF), a ubiquitous solvent in metal–organic framework synthesis, was also used as a probe solvent with similar results. A satisfactory linear

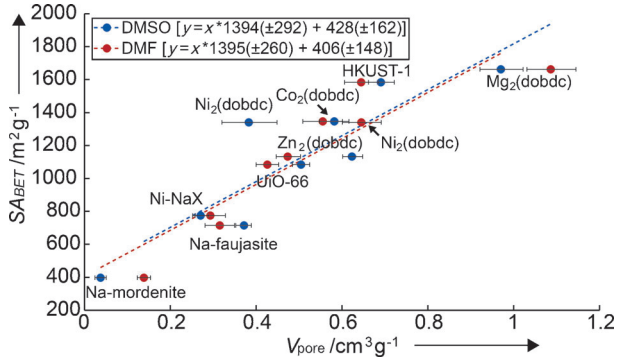

Figure 4. Correlation of BET surface area (SA_{BET}) to the fitted V_{pore} using DMSO and DMF. Dashed lines indicate the fit for each solvent. The error bars encapsulate the ILT error, the pore decay fitting error, and the error in NMR measurement. All samples were tested at RT.

correlation can be found (Figure 4; see Table S1 in the Supporting Information).

The NMR-predicted surface area agrees well with the measured surface area, with the error (±standard deviation) being dominated by the linear regression error that is expected to improve as more frameworks are tested and as the testing method is refined. The analysis clearly distinguishes low-porosity samples from high-surface-area metal–organic frameworks, thus demonstrating its potential for implementation alongside high-throughput synthesis instruments. Also, the flexibility in solvent choice could further simplify sample preparation by enabling testing of as-synthesized frameworks.

A PDE model was developed to further elucidate the physics of a diffusing, heterogeneous framework–solvent system (see the Supporting Information for model details). This model (see Figure S20 in the Supporting Information) utilizes the Bloch–Torrey Equations to compute the evolution of NMR magnetization for a spherically symmetric particle surrounded by varying amounts of bulk solvent. The inversion spectra derived from the analytical model qualitatively match the results found in actual experiments. Furthermore, this model supports the hypothesis that exchanging interfacial solvent produces intermediate relaxation signals. Figure 5

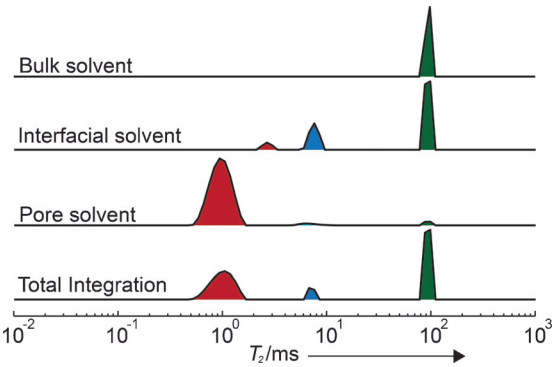

Figure 5. Laplace inversion of T_2 relaxation curves generated by the mathematical model based upon appropriate Bloch–Torrey Equations. Inversions were performed on the separate relaxation signals from the pore solvent, the interfacial solvent, and the bulk solvent, as well as the total signal from all three. Further details on the model and the parameters used can be found in the Supporting Information.

compares the "relaxation spectra" of interfacial solvent with solvent away from the interface. The large intermediate signal in the spectra for interfacial solvent suggests that the interface is indeed an intermediate relaxation environment.

This study has described a robust correlation that relates the surface area of a wide variety of microporous media to the proton relaxation behavior of imbibed solvent, thus demonstrating the potential for NMR relaxometry as a high-throughput screening technique. The results were obtained on a portable NMR instrument that interfaces easily with combinatorial synthesis methods. Simulations using the Bloch–Torrey Equations qualitatively confirm the observed behavior and allow the effects of solvent transport processes to be explored. Further optimization of sample preparation,

measurement methods, and NMR hardware should yield considerable reductions in error and measurement time (see the Supporting Information). The inclusion of this technique in a high-throughput screening workflow is expected to expedite the discovery of new candidate materials for applications such as CO_2 capture.

Received: June 18, 2013
Published online: September 23, 2013

Keywords: high-throughput screening · metal–organic frameworks · microporous materials · NMR relaxometry · NMR spectroscopy

[1] a) S. R. Caskey, A. G. Wong-Foy, A. J. Matzger, *J. Am. Chem. Soc.* **2008**, *130*, 10870 – 10871; b) H. Furukawa, N. Ko, Y. B. Go, N. Aratani, S. B. Choi, E. Choi, A. O. Yazaydin, R. Q. Snurr, M. O'Keeffe, J. Kim, O. M. Yaghi, *Science* **2010**, *329*, 424 – 428; c) J. A. Mason, K. Sumida, Z. R. Herm, R. Krishna, J. R. Long, *Energy Environ. Sci.* **2011**, *4*, 3030; d) T. M. McDonald, D. M. D'Alessandro, R. Krishna, J. R. Long, *Chem. Sci.* **2011**, *2*, 2022; e) A. R. Millward, O. M. Yaghi, *J. Am. Chem. Soc.* **2005**, *127*, 17998 – 17999; f) A. O. Yazaydın, A. I. Benin, S. A. Faheem, P. Jakubczak, J. J. Low, R. R. Willis, R. Q. Snurr, *Chem. Mater.* **2009**, *21*, 1425 – 1430; g) A. O. Yazaydın, R. Q. Snurr, T. H. Park, K. Koh, J. Liu, M. D. LeVan, A. I. Benin, P. Jakubczak, M. Lanuza, D. B. Galloway, *J. Am. Chem. Soc.* **2009**, *131*, 18198 – 18199.

[2] a) J.-R. Li, Y. Ma, M. C. McCarthy, J. Sculley, J. Yu, H.-K. Jeong, P. B. Balbuena, H.-C. Zhou, *Coord. Chem. Rev.* **2011**, *255*, 1791 – 1823; b) K. Sumida, D. L. Rogow, J. A. Mason, T. M. McDonald, E. D. Bloch, Z. R. Herm, T. H. Bae, J. R. Long, *Chem. Rev.* **2012**, *112*, 724 – 781.

[3] a) S. S. Kaye, A. Dailly, O. M. Yaghi, J. R. Long, *J. Am. Chem. Soc.* **2007**, *129*, 14176 – 14177; b) N. Stock, S. Biswas, *Chem. Rev.* **2012**, *112*, 933 – 969; c) E. Biemmi, S. Christian, N. Stock, T. Bein, *Microporous Mesoporous Mater.* **2009**, *117*, 111 – 117.

[4] a) R. Banerjee, A. Phan, B. Wang, C. Knobler, H. Furukawa, M. O'Keeffe, O. M. Yaghi, *Science* **2008**, *319*, 939 – 943; b) N. Stock, T. Bein, *Angew. Chem.* **2004**, *116*, 767 – 770; *Angew. Chem. Int. Ed.* **2004**, *43*, 749 – 752; c) K. Sumida, S. Horike, S. S. Kaye, Z. R. Herm, W. L. Queen, C. M. Brown, F. Grandjean, G. J. Long, A. Dailly, J. R. Long, *Chem. Sci.* **2010**, *1*, 184 – 191.

[5] a) R. Kleinberg, W. Kenyon, P. Mitra, *J. Magn. Reson.* **1994**, *108*, 206 – 214; b) P. J. Barrie, *Annu. Rep. NMR Spectrosc.* **2000**, *41*, 265 – 316; c) R. Brown, P. Fantazzini, *Phys. Rev. B* **1993**, *47*, 14823 – 14834; d) F. D'Orazio, S. Bhattacharja, W. Halperin, K. Eguchi, T. Mizusaki, *Phys. Rev. B* **1990**, *42*, 9810 – 9818; e) S. Davies, K. Packer, *J. Appl. Phys.* **1990**, *67*, 3163 – 3170; f) W. P. Halperin, J. Y. Jehng, Y. Q. Song, *Magn. Reson. Imaging* **1994**, *12*, 169 – 173; g) F. Jaeger, S. Bowe, H. Van As, G. E. Schaumann, *Eur. J. Soil Sci.* **2009**, *60*, 1052 – 1064; h) J. Kärger, R. Valiullin, in *eMagRes*, John Wiley & Sons, Ltd, **2007**; i) W. Kenyon, J. Howard, A. Sezginer, C. Straley, A. Matteson, K. Horkowitz, R. Ehrlich in *Trans. SPWLA Ann. Logging Symp.*, *Vol. 30*, **1989**; j) J. P. Korb, *New J. Phys.* **2011**, *13*, 035016; k) P. McDonald, J. P. Korb, J. Mitchell, L. Monteilhet, *Phys. Rev. E* **2005**, *72*, 11409; l) J. Mitchell, J. D. Griffith, J. H. Collins, A. J. Sederman, L. F. Gladden, M. L. Johns, *J. Chem. Phys.* **2007**, *127*, 234701; m) L. Monteilhet, J. P. Korb, J. Mitchell, P. McDonald, *Phys. Rev. E* **2006**, *74*, 61404; n) H. A. Resing, *Adv. Mol. Relax. Interact. Processes* **1972**, *3*, 199 – 226; o) L. R. Stingaciu, L. Weihermüller, S. Haber-Pohlmeier, S. Stapf, H. Vereecken, A. Pohlmeier, *Water Resour. Res.* **2010**, *46*, W11510; p) R. Valckenborg, L. Pel, K. Kopinga, *J. Phys. D* **2002**, *35*, 249; q) K. Washburn, P. Callaghan, *Phys. Rev. Lett.* **2006**, *97*, 175502.

[6] M. H. Levitt, *Spin dynamics*, Wiley, Chichester, UK **2001**.

[7] K. R. Brownstein, C. Tarr, *Phys. Rev. A* **1979**, *19*, 2446.

[8] a) M. D. Hürlimann, *J. Magn. Reson.* **1998**, *131*, 232 – 240; b) J. Mitchell, T. C. Chandrasekera, M. L. Johns, L. F. Gladden, *Phys. Rev. E* **2010**, *81*, 26101.

[9] a) D. I. Kolokolov, H. Jobic, A. G. Stepanov, J. Ollivier, S. Rives, G. Maurin, T. Devic, C. Serre, G. Férey, *J. Phys. Chem. C* **2012**, *116*, 15093 – 15098; b) T. Ueda, K. Kurokawa, Y. Kawamura, K. Miyakubo, T. Eguchi, *J. Phys. Chem. C* **2012**, *116*, 1012 – 1019; c) M. Wehring, J. Gascon, D. Dubbeldam, F. Kapteijn, R. Snurr, F. Stallmach, *J. Phys. Chem. C* **2010**, *114*, 10527 – 10534.

[10] a) P. C. Hansen, *SIAM Rev.* **1992**, *34*, 561 – 580; b) J. Mitchell, T. C. Chandrasekera, L. F. Gladden, *Prog. Nucl. Magn. Reson. Spectrosc.* **2012**, *62*, 34 – 50; c) S. W. Provencher, *Comput. Phys. Commun.* **1982**, *27*, 213 – 227; d) L. Venkataramanan, Y. Q. Song, M. D. Hurlimann, *IEEE Trans. Signal Proces.* **2002**, *50*, 1017 – 1026.

[11] a) B. Blümich, J. Perlo, F. Casanova, *Prog. Nucl. Magn. Reson. Spectrosc.* **2008**, *52*, 197 – 269; b) G. Eidmann, R. Savelsberg, P. Blümler, B. Blümich, *J. Magn. Reson.* **1996**, *122*, 104 – 109; c) J. Perlo, F. Casanova, B. Blumich, *J. Magn. Reson.* **2005**, *176*, 64 – 70.

[12] a) H. Carr, E. Purcell, *Phys. Rev.* **1954**, *94*, 630 – 638; b) S. Meiboom, D. Gill, *Rev. Sci. Instrum.* **1958**, *29*, 688 – 691.

[13] P. D. Dietzel, B. Panella, M. Hirscher, R. Blom, H. Fjellvag, *Chem. Commun.* **2006**, 959 – 961.

[14] J. H. Cavka, S. Jakobsen, U. Olsbye, N. Guillou, C. Lamberti, S. Bordiga, K. P. Lillerud, *J. Am. Chem. Soc.* **2008**, *130*, 13850 – 13851.

